SMAR 2015 – Third Conference on Smart Monitoring,
Assessment and Rehabilitation of Civil Structures

SMAR 2015

Innovative Precast Hollow-Core FRP-Concrete-Steel Bridge Columns Subjected to Vehicle Collision

Omar I. Abdelkarim[1], and Mohamed A. ElGawady[2]

[1] Ph.D. Candidate, Missouri University of Science and Technology, Rolla, MO, USA
[2] Benavides Associate Professor, Missouri University of Science and Technology, Rolla, MO, USA

ABSTRACT: This paper investigates the behavior of innovative accelerated bridge construction system of hollow-core fiber reinforce polymer (FRP)-concrete-steel columns (HC-FCSs) under vehicle collision using LS-DYNA software. The dynamic behavior of HC-FCS columns was compared to the dynamic behavior of reinforced concrete (RC) column under vehicle collision. The HC-FCS column consists of a concrete wall sandwiched between an outer FRP tube and an inner steel tube. The steel tube works as longitudinal and transversal reinforcements. The FRP tube only confines the sandwiched concrete. The FRP tube protects the concrete from spalling because of the confinement. Ford Single Unit Truck (SUT) collided with a HC-FCS column and a reinforced concrete column with different velocities. The HC-FCS column and the RC column have the same flexural strength. Each column was collided with three different velocities of 112 kph, 80 kph, and 32 kph. The PDFs were calculated and compared for each case. The PDF values of the HC-FCS columns were lower than those of the RC column by approximately 28% - 39% when they were collided with vehicles having velocities ranging from 80 kph to 112 kph. However, the PDF of the RC and HC-FCS columns were almost the same when they were collided with vehicle’s velocity of 32 kph.

1 INTRODUCTION

Accidents can have serious repercussions with regard to both human life and transportation systems. Many vehicle collision events involving bridge piers have been reported throughout the US. These collisions often result in either a complete or a partial bridge collapse (Harik et al. 1990). For example, in May of 2013, two trains collided at a rail intersection just outside of Scott City in southeast Missouri. Numerous train cars were derailed, and seven people were injured. The derailed cars hit a highway overpass, causing it to collapse. The preliminary estimated cost for replacing the overpass was approximately $3 million (McGrath 2013).

Numerous researchers have used LS-DYNA software to investigate the modeling of concrete columns under extreme loading (Abdelkarim and ElGawady 2014). El-Tawil et al. (2005) used LS-DYNA software to examine two bridge piers impacted by different trucks at different velocities. The peak dynamic force (PDF: the maximum contact force of the vehicle collision on the bridge column) was evaluated. Buth et al. (2011) experimentally studied the collision of tractor-trailers into a rigid column that was constrained at both ends. Numerical models were used to conduct a parametric study on single unit truck (SUT) using LS-DYNA software. The investigated parameters included the pier's diameter, the vehicle's weight, the vehicle's velocity, and the cargo's state (rigid versus deformable). Abdelkarim and ElGawady (2015) have investigated the behavior of the reinforced concrete columns under vehicle collision.

Hollow-core concrete columns are often used for tall bridge columns in moderate to high seismic regions such as New Zealand, Japan, and Italy to reduce the column's mass which reduces the bridge self-weight contribution to the inertial force during an earthquake. Hollow-core columns also result in reduced foundation dimensions which reduce substantially the construction cost.

Montague (1978) developed an innovative double-skin tubular column (DSTC). These columns consist of concrete wall sandwiched between two generally concentric steel tubes. More recently, Teng et al. (2004) used fiber reinforced polymers (FRP) as an outer tube and the steel as an inner tube in the double-skin tubular elements. This system combines and optimizes the benefits of all three materials: FRP, concrete, and steel in addition to the benefits of the hollow-core concrete columns to introduce hollow-core FRP-concrete-steel columns (HC-FCS). Few investigators studied the behavior of the HC-FCS columns. HC-FCS displayed high concrete confinement and ductility. Abdelkarim and ElGawady (2014) investigated numerically the behavior of the HC-FCS columns under the combined axial and lateral loading through an extended parametric study.

However, several studies investigated the behavior of the reinforced concrete bridge columns under vehicle collision; very few studies investigated the behavior of other types of bridge columns under vehicle collision. This paper used finite element analysis to investigate the behavior of the hollow-core FRP-concrete-steel (HC-FCS) columns comparable to the behavior of the RC columns under vehicle collision.

2 FE MODEL VALIDATION

Experiments conducted on vehicle collisions with concrete columns are both difficult and expensive. Finite element analysis (FEA) is considered an attractive approach because it is economical, reliable, and easy to implement. The FEA of a collision event requires a combination of vehicle and concrete structure modeling.

Bridge pier models similar to the one used by El-Tawil et al. (2005) was developed during the course of this study. The models were subjected to the impact loads similar to those used by El-Tawil et al. (2005). The results from El-Tawil et al. (2005) were used to validate the developed models. In these models, the bridge pier was 9,925 mm tall (see Fig. 1) and it was supported by a reinforced concrete pile cap that was 3,300 mm x 2,300 mm x 1,075 mm. The pile cap was supported by six prestressed piles that were 450 mm in diameter and 10,000 mm in length.

Fully integrated 8-node brick elements, with elastic material (mat. 001), were used to simulate the substructure (pier and pile cap). Beam truss elements were used to model all of the reinforced bars. These elements shared nodes with the concrete elements. The piles were simulated with beam element type and were supported by four discrete lateral spring elements. These elements were modeled by a spring inelastic material (mat. S08). This material provided a compression response only. Bowles' equations (1988) for soil's compressive stiffness were used to calculate the modulus of the subgrade's reaction to the soil. The springs were spaced 440 mm apart.

The bridge superstructure was composed of a composite steel-concrete box girder. Thirty-six Belytschko-Schwer resultant beam-type elements were used to simulate two adjacent steel girders. This superstructure's transformed steel cross-sectional area was 80,000 mm^2. The strong moment of inertia (the Iyy about the vertical axis) was 8.3 x 10^{10} mm^4, and the weak moment of inertia (the Izz about the horizontal axis) was 2.8 x 10^{10} mm^4. The superstructure's two unequal spans were 53,340 mm and 50,290 mm. This superstructure was assumed to be pinned at the far ends. The Hughes-Liu beam-type element was used to simulate the bridge bearings located under the superstructure. These bearings were 37 mm thick and 200 mm x 200 mm in the cross-section. The bridge bearing's shear modulus was 0.61 MPa.

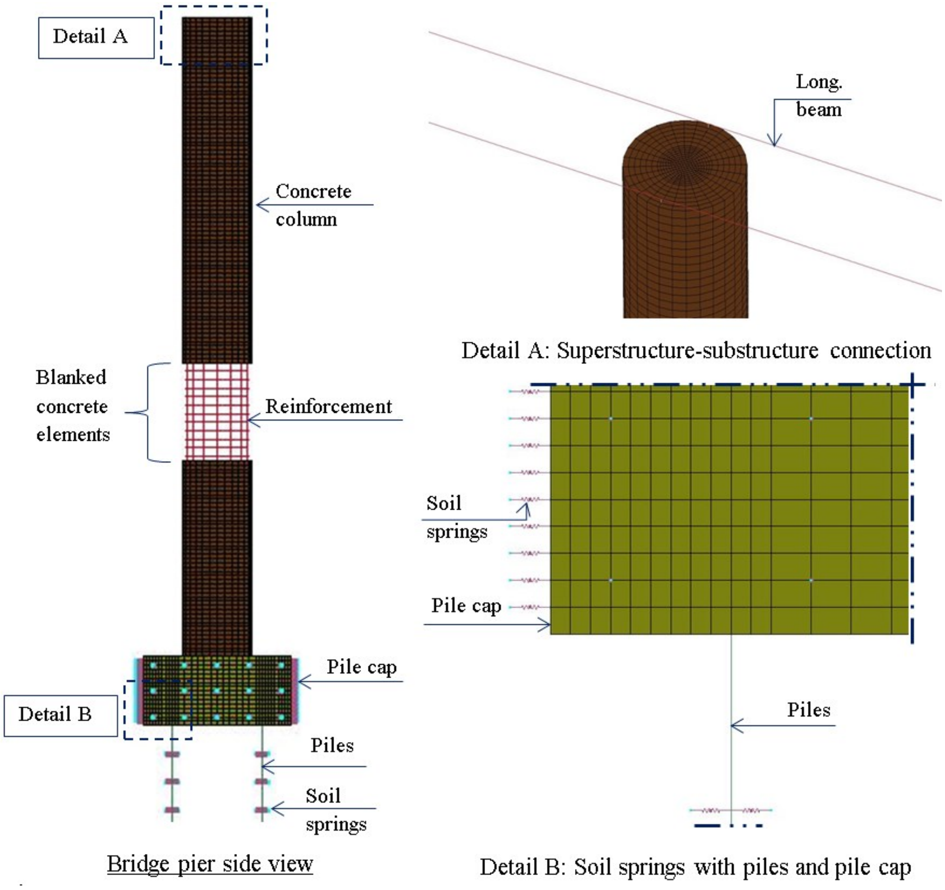

Figure 1. Components of the FE model for validation against El-Tawil's et al. results (2005)

A Chevrolet pickup's reduced finite element model was used to study the vehicle's collision with a bridge pier. A surface-to-surface contact element was used between the vehicle and the bridge pier in the finite element models; the coefficient of friction was 0.3. The vehicle model was developed by the National Crash Analysis Center (NCAC) of The George Washington University under a contract with both the Federal Highway Administration (FHWA) and the National Highway Traffic Safety Administration (NHTSA) of the U.S. Department of Transportation (DOT).

The collision event of the Chevrolet pickup with the bridge pier, at a velocity of 110 kph, at a time of 0.05 seconds is illustrated in Fig. 2(a). The FE results from this study, in general, were close to the results reported by El-Tawil et al. (2005), as illustrated in Fig. 2(b). The percentages of difference between the PDFs from this study and those from the El-Tawil et al. (2005) study for vehicle velocities of 55 kph, 110 kph, and 135 kph were between 0.6% and 9.2% (Fig. 2b). These differences occurred as a result of the number of uncertainties such as a column's concrete cover, mesh size, the column component's material models, the vehicle nose's location at the column's face, and the values of modulus of the subgrade's reaction of the soil springs. These parameters were not accurately described in El-Tawil et al. (2005).

The percentages of difference between the ESFs from this study and those from the El-Tawil et al. (2005) study for vehicle velocities of 55 kph, 110 kph, and 135 kph were between 6.4% and 14.5% (Fig. 2b).

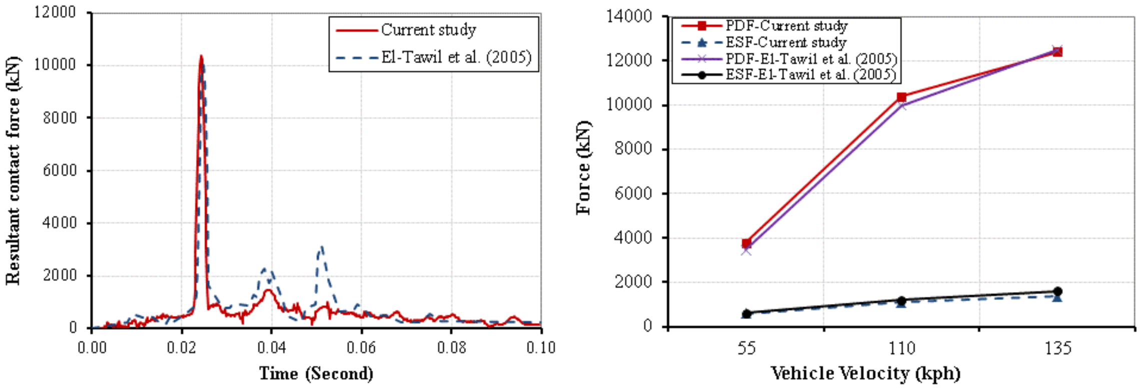

(a) ((b)

Figure 2. Current study FE results versus El-Tawil et al. (2005) FE results; (a) Impact force when vehicle's velocity was 110 kph and (b) PDF and ESF versus the vehicle velocities.

3 FE MODELING

The FE models were conducted on LS-DYNA software. The columns investigated in this study were supported on a concrete footing which had fixed boundary condition at its bottom. All of the columns had superstructure attached at its top as explained in the validation section. Each column had an outer diameter (D_o) of 1.5 m and a height (H) of 7.5 m with span-to-depth ratio of 5 (Fig. 3). The soil depth above the top of the footing (d_s) was 1.0 m. Both the RC and HC-FCS columns were designed to have the same flexural strength. The longitudinal steel reinforcement of the RC column was 24 Ø 35 representing to 1.25% of the concrete cross-sectional area. The RC column's hoop reinforcement was 5 Ø 16. The outer FRP tube thickness of the HC-FCS column was 7.6 mm. The outer diameter of the inner steel tube (D_i) was 1.0 m and its thickness was 6.4 mm. The diameter-to-thickness of the steel tube was 157. The inner steel tube was extended inside the footing using an embedded length (L_e = 1.6 D_i) while the FRP tube was stopped at the top of the footing. The steel tube was hollow inside. The HC-FCS column did not include any shear or flexure reinforcement except the steel tube. Table 1 summarizes the columns' characteristics.

Table 1: Summary of the examined columns' characteristics

Column	Diameter (m)	Height (m)	Steel tube/reinforcement		FRP tube	
HC-FCS column	1.5	7.5	Diameter (m)	1.0	Diameter (m)	1.5
			Thickness (mm)	6.4	Thickness (mm)	7.6
RC column	1.5	7.5	Rebars	24 Ø 35	N.A.	

Modeling of the RC column is as explained in the validation section. For the HC-FCS column, one-point quadrature solid elements were used to model the sandwiched concrete. An hourglass control was used to avoid spurious singular modes (e.g., hourglass modes). The hourglass value for each of the models was taken as the default value 0.10, with an hourglass control type_4 (Flanagan-Belytschko stiffness form). Contact elements surface-to-surface were used to simulate the interface between the concrete column and the FRP tube. They were also used between the concrete column and the steel tube. This type of contact considers slip and separation that occurs between master and slave contact pairs. Hence, slip/debonding will be displayed if either occurs between the concrete wall's surface and the tube's surface. This type of contact was used also between the concrete footing and the steel tube. Node-to-surface contact elements were used between the bottom edges of the FRP tube and the steel tube, and the concrete footing. The coefficient of friction for all of the contact elements was taken as 0.6.

The AASHTO-LRFD considers vehicle impact to be an extreme load. Therefore, a column's nonlinear behavior is both expected and allowed. Hence, a nonlinear concrete material model (mat72RIII) was used for all columns and footings in this study. The concrete unconfined compressive strength (f_c') was taken 34.5 MPa. The column's concrete cover was designed to spall at an axial compressive strain exceeding 0.005 (Caltrans 2006).

An elasto-plastic constitutive model, mat003-plastic_kinamatic, was used for steel tube. The following parameters were needed to define this material model: the elastic modulus (E), the yield stress, and Poisson's ratio. These parameters were assigned the following values: 200 GPa, 420 MPa, and 0.30, respectively (Caltrans 2006).

The FRP material used was modeled as an orthotropic material using "002-orthotropic_elastic" material. This material is defined by several engineering constants: elastic modulus (E), shear modulus (G), and Poisson's ratio (PR), in the three principle axes (a, b and c). The fiber orientation is defined by a vector. The following characteristics, based on the manufacturer "Grace Composites and FRP Bridge Drain Pipe" were implemented in the FE. The elastic modulus in the hoop direction (Ea), shear modulus in the transverse direction (Gab), and Poisson's ratio of the FRP tube were 20.8 GPa, 277 MPa, and 0.35, respectively. The failure criterion for the FRP, defined as "000-add_erosion," was assigned the ultimate strain of FRP in "EFFEPS" card. The ultimate tensile strain in the hoop direction was 0.013.

Loading strain rates may play an essential role in a structure's response. The dynamic increase factor (DIF) is typically used to describe the increase in the material strength under dynamic loading. The model of Malvar and Ross (1998) was considered for the strain rate effect on the concrete material. The Cowper-Symonds's model was adopted for the strain rate effect on the material of steel. The model of Gama and Gillespie (2011) was considered for the strain rate effect of the FRP material. The strain rate effect was considered for the RC and HC-FCS columns.

The RC and HC-FCS columns were collided with a Ford F800 single unit truck (SUT; Fig. 4). Each column was collided with three different velocities of 112 kph, 80 kph, and 32 kph. The mass of the vehicle was 8 tons. Automatic_surface_to_surface contact elements by parts with the contact factor SOFT=1 were used between the vehicle and the column. The algorithm Automatic_surface_to_surface is a penalty-based which was designed to examine each slave node for penetration through the master surface at every time step. So, if any penetration was found between the parts in contact, a nominal interface spring would apply a force proportional to the penetration depth of these interfaces to eliminate the penetration. The distance between the vehicle's nose and the column's face was taken as 150 mm.

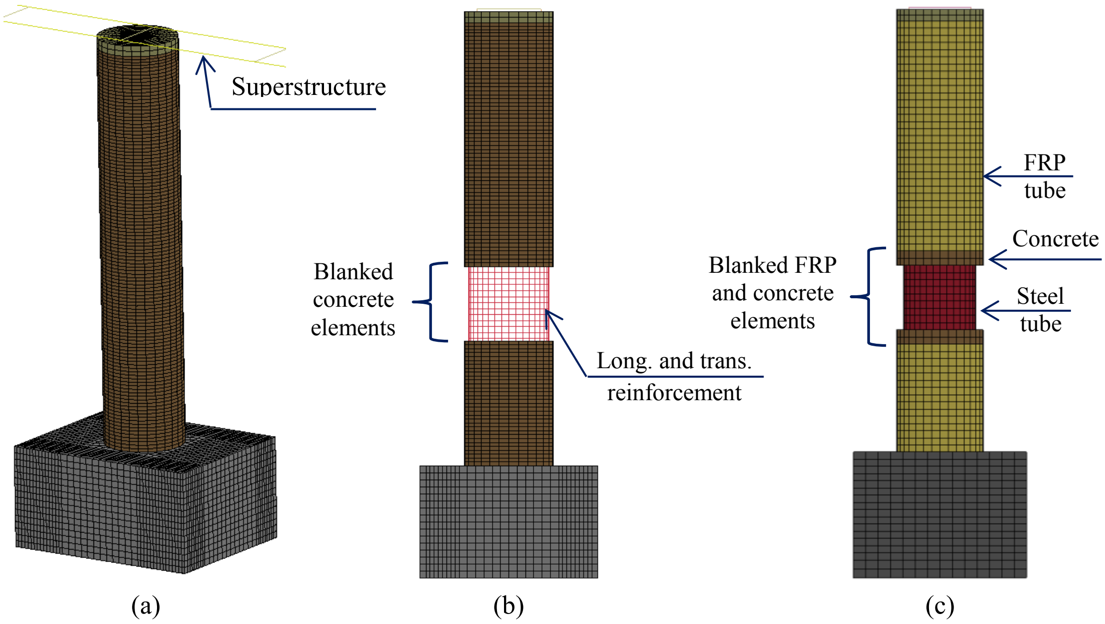

Figure 3. Columns FE modeling: (a) 3D view, (b) RC-column, and (c) HC-FCS column

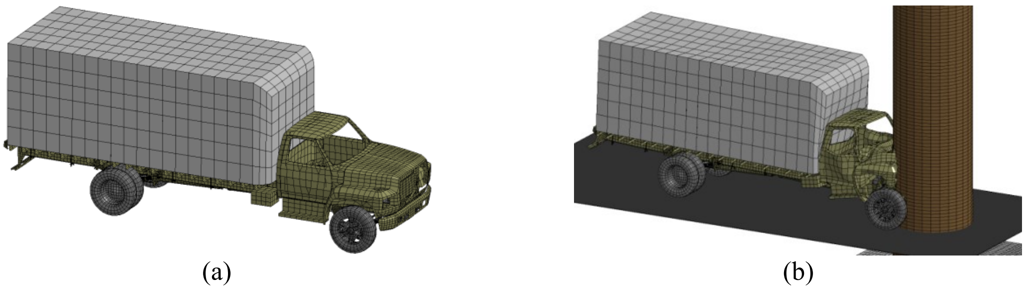

Figure 4. (a) FE model of the FORD F800-SUT and (b) Vehicle collision with the column

4 RESULTS AND DISCUSSION

The PDFs of the HC-FCS and RC columns collided with vehicle's velocity of 112 kph were 6,802 kN and 11,167 kN, respectively (Fig. 5a). The PDF of the HC-FCS column was lower than that of the RC column by approximately 39% when it was collided with a vehicle's velocity of 112 kph. The PDFs of the HC-FCS and RC columns collided with vehicle's velocity of 80 kph were 2,806 kN and 3,898 kN, respectively (Fig. 5b). The PDF of the HC-FCS column was lower than that of the RC column by approximately 28% when it was collided with a vehicle's velocity of 80 kph. The PDFs of the HC-FCS and RC columns collided with vehicle's velocity of 32 kph were 1,740 kN and 1,722 kN, respectively (Fig. 5c). The PDFs of the HC-FCS and RC columns were almost the same when it was collided with a vehicle velocity of 32 kph.

The concrete spalling occurred during the vehicle collision with the RC column because of the high local strain (Fig. 6a). However, the FRP tube in the HC-FCS column protected the concrete from spalling and increased the ultimate compressive strain by approximately 5 times than that of the RC column (Fig. 6b).

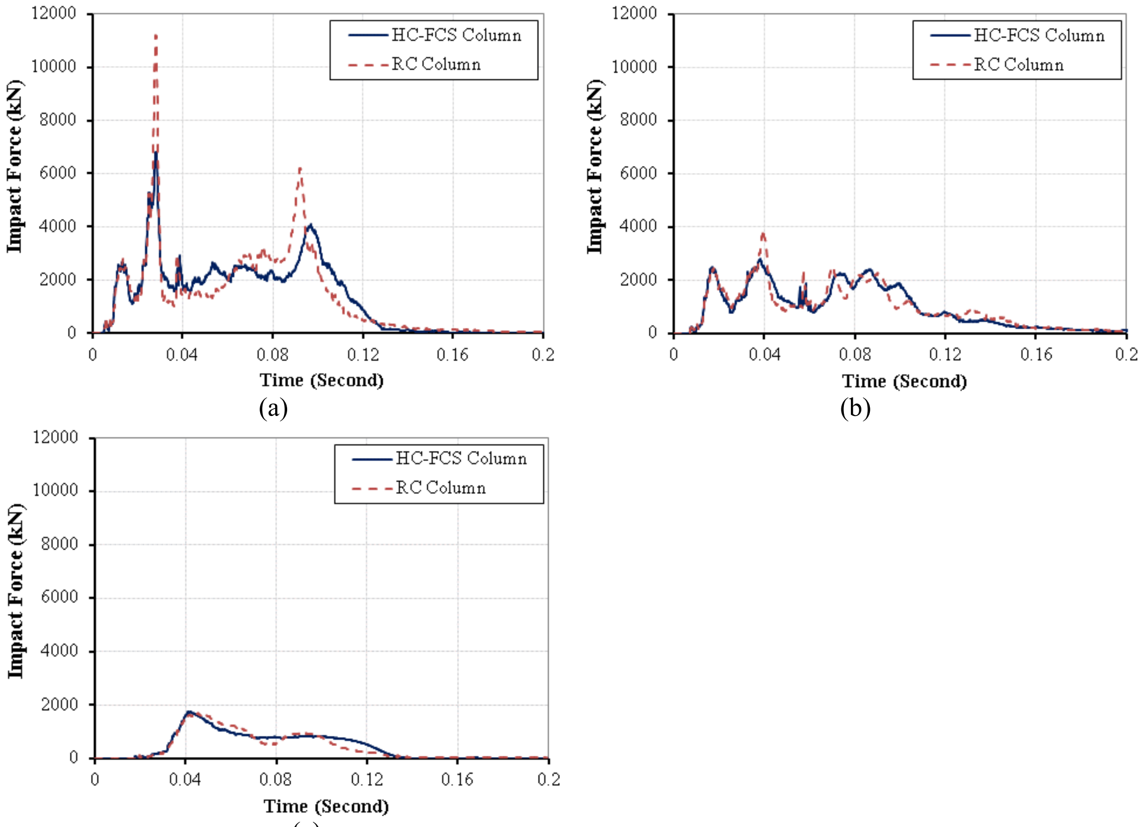

Figure 5. Time vs impact force for HC-FCS column and RC column under vehicle collision with a velocity of: (a) 112 kph, (b) 80 kph, and (c) 32 kph

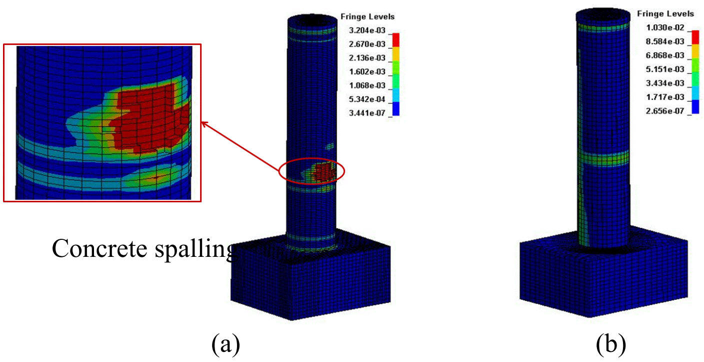

Figure 6. Column strain countour: (a) RC Column, and (b) HC-FCS column

5 CONCLUSIONS

The dynamic behavior of the HC-FCS columns was compared to the dynamic behavior of the RC columns under vehicle collision. Each column was collided with three different velocities of 112 kph, 80 kph, and 32 kph. The PDFs were calculated and compared for each case. The PDF values of the HC-FCS columns were lower than those of the RC column by approximately 28% - 39% when they were collided with vehicles having velocities ranging from 80 kph to 112 kph. The vehicles mass was 18 kips. The PDFs of the HC-FCS and RC columns were approximately equal when they were collided with a vehicle having velocity of 32 kph. Concrete spalling occurred during the vehicle collision with the RC column because of high local strains. However, the FRP tube in the HC-FCS column protected the concrete from spalling and increased the ultimate compressive strain by approximately 5 times than that of the RC column.

6 ACKNOWLEDGEMENT

This research was conducted by Missouri University of Science and Technology and was supported by Missouri Department of Transportation (MoDOT) and Mid-American Transportation Center (MATC). The authors also appreciate the support from the National University Transportation Center (NUTC) at Missouri University of Science and Technology (Missouri S&T). However, any opinions, findings, conclusions, and recommendations presented in this paper are those of the authors and do not necessarily reflect the views of the sponsors.

REFERENCES

AASHTO, (2012), AASHTO-LRFD Bridge Design Specifications – Customary US Units, sixth edition, Washington, DC.

Abdelkarim, O. and ElGawady, M. (2015). “Impact Analysis of Vehicle Collision with Reinforced Concrete Bridge Columns.” Trans. Research Board (TRB) conf. (2015), Washington Dc, 15-4461.

Abdelkarim, O. and ElGawady, M. (2014). "Analytical and Finite-Element Modeling of FRP-Concrete-Steel Double-Skin Tubular Columns." J. Bridge Eng., 10.1061/(ASCE)BE.1943-5592.0000700 , B4014005.

Bowles, J. (1988). “Foundation Analysis and Design.” McGraw-Hill Inc., USA, 1004 pp.

Buth, C. E., Brackin, M. S., Williams, W. F., and Fry, G.T. (2011). “Collision Loads On Bridge Piers: Phase 2.” Texas Dept. of Trans. Research and Technology Implementation Office, Report 9-4973-2.

California Department of Transportation. (2006). “Seismic Design Criteria”. California Department of Transportation, Rev. 1.4.

Comité Euro-International du Béton. (1993). “CEB-FIP Model Code 1990.” Redwood Books, Trowbridge, Wiltshire, UK.

Cowper, G. R. and Symonds, P. S. (1957). “Strain Hardening and Strain Rate Effects in Impact Loading of Cantilever Beams.” Brown University, App. Math. Report No. 28.

El-Tawil, S., Severino, E., and Fonseca, P. (2005). “Vehicle Collision with Bridge Piers.” J. Bridge Eng., 10(3), 345-353.

Eurocode 1: Actions on structures – Part 1-1: General actions – Densities, self-weight, imposed loads for buildings, Final Draft prEN 1991-1-1, October 2002.

Gama, BA., Gillespie, JW. (2011). “Finite element modeling of impact, damage evolution and penetration of thick-section composites.” International Journal of Impact Engineering, 38 (4), pp. 181-197.

Harik, I., Shaaban, A., Gesund, H., Valli, G., and Wang, S. (1990). ”United States Bridge Failures, 1951–1988.” J. Perform. Constr. Facil., 4(4), 272–277.

LS-DYNA; theory manual for version 971. (2006). Livermore Software Technology Corporation.

Malvar, L. J. and Ross, C. A. (1998). “Review of Strain Rate Effects for Concrete in Tension.” ACI Materials Journal, 95, 735-739.

McGrath, J. J. (2013). “Replacement of Missouri Route M Overpass Creamed by Freight-Train Crash in Scott County Estimated to Cost about $3 Million: Accident is the Third Railroad Mishap in Four Months in Rockview- May 26, 2013” International Business times, http://www.ibtimes.com/replacement-missouri-route-m-overpass-creamed-freight-train-crash-scott-county-estimated-cost-about, Accessed by July, 2014.

Montague, P., (1978). “Experimental behavior of double-skinned, composite, circular cylindrical-shells under external-pressure”. Journal of Mechanical Engineering Science, 20(1), pp. 21–34.

Teng, J.G., Yu, T., and Wong, Y.L. (2004). “Behavior of Hybrid FRP-Concrete-Steel Double-Skin Tubular Columns.” Proc. 2nd Int. Conf. on FRP Composites in Civil Engineering, Adelaide, Australia, 811-818.